DESIGN, FABRICATION, AND TESTING OF A LIQUID NITROGEN-COOLED ALUMINUM INDUCTOR

R. C. Zowarka

Presented at the
4th IEEE International Pulsed Power Conference
Albuquerque, New Mexico
June 6-8, 1983

Publication No. PN-92
Center for Electromechanics
The University of Texas at Austin
Balcones Research Center
EME 1.100, Building 133
Austin, TX 78758-4497
(512)471-4496

DESIGN, FABRICATION, AND TESTING OF A
LIQUID NITROGEN-COOLED ALUMINUM INDUCTOR

R. C. Zowarka
Center for Electromechanics
The University of Texas at Austin
Taylor Hall 167
Austin, TX 78712

Summary

In July 1981, a joint project between the Center for Electromechanics and the General Dynamics Corporation was undertaken to accelerate the first metallic penetrator-type projectile by means of an electromagnetic railgun. A preliminary design effort at CEM-UT indicated the feasibility of driving a railgun with the CEM-UT 10-MJ homopolar generator charging an energy storage inductor. Several system options were presented to General Dynamics, and a liquid nitrogen-cooled aluminum Brooks coil inductor charged with the 10-MJ HPG was selected. This paper describes the design, fabrication, and testing of the inductor. A scale model of the system was constructed during the design phase, and the circuit parameters were measured. These parameters were scaled up to the full-size system and are compared to actual circuit parameters measured while testing the coil.

Introduction

In 1978 the Department of Defense (DoD) initiated a national program to assess and advance the state of electromagnetic propulsion technology. In conjunction with this effort, the Office of the Secretary of Defense organized a technical workshop of sixty scientists and engineers to review recent developments in underlying support technologies. The applicability of electromagnetic propulsion (EM) to gun and launch systems became evident. The DoD working group on EM undertook the coordination of the military service interests. As part of this initial effort, General Dynamics started work on the acceleration of the first metallic penetrator-type projectile with an EM railgun. In July 1981 a preliminary design effort at the Center for Electromechanics at The University of Texas at Austin (CEM-UT) indicated the feasibility of driving a railgun with the CEM-UT 10-MJ homopolar generator (HPG) charging an energy storage inductor. Several system options were presented to General Dynamics, and a cryogenic Brooks coil inductor charged with the 10-MJ HPG was selected. At the same time, responsibility for design and construction of the system components was determined. General Dynamics would design and build the opening switch, the railgun, and the projectile catch tank. CEM-UT would design and construct the Brooks coil inductor and shielding, the system busbars, and a means for protecting the HPG from large voltage transients. The system components were installed, and testing began in August 1982. The first successful acceleration of the Phalanx-shaped projectile with the EM railgun took place in September 1982. To date, the 85-g projectile has been accelerated to 600 m/s.

Experiment Definition and Preliminary Analysis

The project was initiated by examining different EM gun program options. These options centered around the inductor design. A simple circuit model shown in Fig. 1 was used to analyze several system options.

The Brooks coil option was examined because it would give the largest value of inductance for a given amount of material. Further gains in energy storage would then be realized by cooling the coil to liquid nitrogen temperature. The indicated system performance is presented in Table 1.

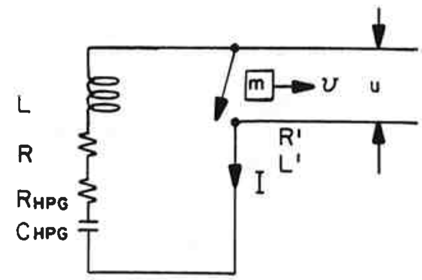

C_{HPG} = equivalent HPG capacitance
R_{HPG} = HPG resistance
R = resistance of coil and buswork
L = inductance of energy storage coil
R´ = resistance per unit length of rail
L´ = inductance per unit length of rail
M = mass of projectile
v = projectile velocity
U = arc voltage drop
I = current

Fig. 1. HPG railgun circuit model

Table 1. Brooks coil system option

HPG Parameters: Stored energy 6.8 MJ
Voltage 42.4 V
Resistance 18.8 μΩ

L_i, μH	R_i, μΩ	I, kA	E, MJ	R_{ckt}, μΩ	Proj. Mass, g	Gun Length, m	Proj. Velocity, km/s
13	5	612	2.4	28.8	30	4	3.7
"	"	"	"	"	85	4	2.2
"	"	"	"	"	85	30	3.1

The decision was made to build the cryogenic Brooks coil inductor within a shield to gain experience in operating cryogenic energy storage coils.

Brooks Coil

In a Brooks coil,[1] the following simple relations exist among the principal coil dimensions (Fig. 2):

Side of square cross section = c
Inner diameter of winding = 2c
Mean diameter of a turn = 3c = 2a
Outer diameter of winding = 4c.

The inductance of a Brooks coil is given by the simple formula

$$L = 0.016994\ a\ N^2$$

where L = coil inductance, μH
a = mean coil radius, cm
N = number of turns.

greater than its dc resistance.

Table 3 shows values of the Table 2 parameters as functions of N, the number of turns in the coil.

Table 3. Evaluation of Brooks Coil Formulas

N	a, cm	c, cm	c/N,* cm	R,† μΩ	J, kA/cm^2	M, kg	R_{init},§ μΩ	
4.7	34.6	23.1	4.9	3.86	6.61	314	5.3	Coil
4.8	33.2	22.1	4.6	4.20	7.35	277	5.2	too
4.9	31.9	21.2	4.3	4.56	8.15	244	5.1	heavy
5.0	30.6	20.4 (8 in.)	4.1	4.94	9.01	217	5.0	
5.1	29.4	19.6	3.8	5.35	9.95	192	4.8	Res-
5.2	28.3	18.9	3.6	5.78	10.96	171	4.7	ist-
5.3	27.2	18.2	3.4	6.24	12.06	153	4.5	ive-

Note: Values in this table were calculated by choosing a value for N and computing a, c, r, J, and M using a N^2 = 765 (Table 2)

* Conductor thickness per turn
† Actual dc resistance from Eqn. 3, Table 2
§ Required initial resistance to deliver 750 kA, taking conductor temperature rise into account

It can be seen from Table 3 that a 5-turn coil meeting the Brooks coil requirements of Table 2 has the proper initial resistance to allow charging to 750 kA. Fewer turns lead to a more massive coil, while more turns result in too high an initial resistance. In the latter case, the coil could not be charged to 750 kA due to the increasing resistance associated with temperature rise in the conductor.

Making the assumption that the current can be fed into the 13-μH inductor in 0.4 s in a 1/4 sine wave of current vs time, the effect of skin depth for the conductor can be found as a function of time. The curves in Fig. 4 show the resistance ratio computed for cryogenic aluminum for the three different thicknesses. Using a 1.27-cm (1/2-in.) thick conductor, the effect is negligible.

From Table 3 it can be seen that a 5-turn coil with a conductor thickness of 4.1 cm (1.6 in.) and a principal dimension of C = 8 in. (see Fig. 2) is required skin depth considerations, the coil conductor should be 1.27 cm (0.5 in.) thick. Therefore, the coil will be a 3-start, 5-turn coil made of 6101-T61 aluminum busbar

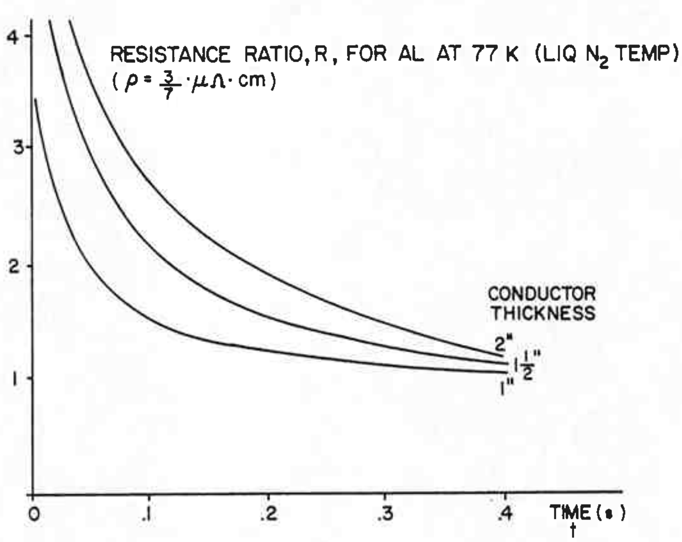

Fig. 4. Skin effect curves

stock 8-in. wide and 1/2 in. thick (Fig. 5). The coil is capable of accepting a charge of 750 kA. The inductance of this geometry is 13 x 10^{-6} H.

Preliminary Mechanical Analysis

The stresses in this coil arise from two main effects, pinch pressures generated in the coil windings and bursting forces on the loop. The coil cross section is a 20.3-cm (8-in.) square. If this cross section is replaced with a 22.9-cm (9-in.) diameter circle

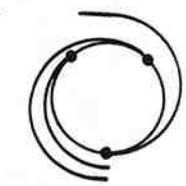

Fig. 5. Brooks coil winding pattern

with the total current of 5 x 750 kA flowing in a thin ring at its surface, then the pinch pressure on the conductors is

$$P = \frac{B^2}{2\mu_0}$$

where P = pinch pressure
B = magnetic flux density
μ_0 = permeability of air.

Substituting,

$$B = \frac{\mu_0 I}{2\pi r}$$

and the pressure becomes

$$P = \frac{\mu_0 I^2}{8\pi^2 r^2} = 1.71 \times 10^7 \ \mathrm{N \cdot m^{-2}} \ (2{,}485 \text{ psi}).$$

The burst pressure may be computed by obtaining the increase of energy contained in the coil by imagining it to be increased in size by some convenient amount and then equating this energy change to an equivalent radial pressure times the associated volume change:

$$1/2(L_f i^2 - L_i I^2) = P\Delta V.$$

$$P = 3.07 \times 10^7 \ \mathrm{N/m^2} \ (4{,}454 \text{ psi}).$$

An estimate of the hoop stress can then be calculated by assuming the coil conductors to be a thin-wall pressure vessel.

$$\sigma_t = \frac{PD}{2t} = \frac{3.07 \times 10^7 \times 24}{2 \times 8}$$

$$= 4.61 \times 10^7 \ \mathrm{N/m^2} \ (6{,}681 \text{ psi}).$$

This stress is close to the yield stress in 6000 series aluminum in the H condition. The calculation is approximate, however. Furthermore, the coil will be wrapped in a spiral configuration, and this is not the same as a solid-wall pressure vessel. The coil will have to be banded. As the coil cools in the liquid nitrogen, the aluminum will have a larger coefficient of thermal expansion than the glass banding. For this reason, the banding was pretensioned during application so that the cured banding ring would maintain contact with the coil as the coil-banding system was cooled. Because the inner layers of banding were in compression and the outer layers were probably close to being unloaded due to the loss of tension during cure, the

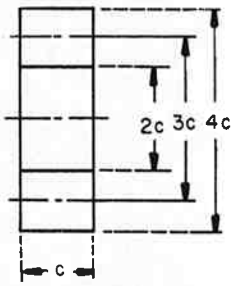

Fig. 2. Brooks coil cross section

A shortcoming of the Brooks coil design is that it must be placed in a magnetic shield structure to lower the magnetic flux seen in the laboratory during discharge.

The on-axis and in-plane fields of the coil at a full current of 750 kA x 5 turns are shown in Fig. 3.

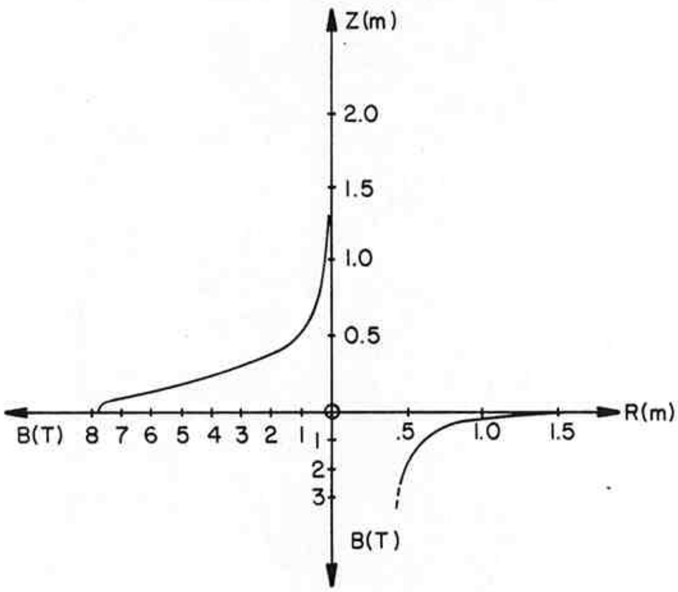

Fig. 3. Coil flux density distribution

Electrical Analysis[2]

The starting point for the preliminary design is to assume a certain efficiency of energy transfer from the HPG to the inductor. Optimization studies show this value to be in the neighborhood of 36 percent for this machine configuration.[3] At design speed the HPG stores 10 MJ. The maximum current the generator can deliver to a similar load impedance is known from experiments to be 750 kA. From these values, a reasonable starting value for coil inductance can be calculated:

$$L = \frac{2 \times (\text{Energy transfer efficiency}) \times (\text{HPG energy})}{I_{max}^2}$$

$$= \frac{2 \times (0.36) \times (10^7 \text{ J})}{(750{,}000 \text{ A})^2}$$

$$\cong 13 \times 10^{-6} \text{ H}.$$

A set of parametric equations describing the Brooks coil design is given in Table 2.

The equivalent capacitance of the generator at full field excitation is $C = (4\pi^2 J/\phi^2) = 7{,}864$ F

where C = capacitance, F
J = rotor moment of inertia (64.04 N•m•s^2)
ϕ = flux linking the rotor (0.567 Wb).

Table 2. Brooks Coil Formulas

1. $L = 0.017aN^2$, μH
2. $c = 2a/3$, cm
3. $R = \frac{\rho\ \ell}{A} = \frac{2\pi\rho N^2 a}{c^2} = 2.69\ N^2 \frac{a}{c^2}$, μΩ
4. $J = \frac{IN}{c^2}$, A/cm^2
5. $M = 2\pi w a c^2 = 17\ ac^2$, grams

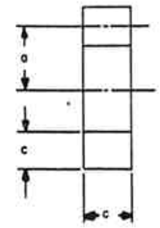

where L = coil inductance (13×10^{-6} H)
I = peak current (750,000 A)
ρ = resistivity of conductor material (3/7 μΩ•cm)
w = density of conductor material (2.7 g/cm^3)
R = coil resistance, μΩ
a, c = coil dimensions, cm
J = peak current density, A/cm^2
M = coil weight, g
N = number of turns in coil

The design speed for the generator is 560 rad/s (5,350 rpm). A realizable discharge speed would be 524 rad/s (5,000 rpm). The open-circuit voltage of the generator at this speed is

$$V_{oc} = \frac{\omega\phi}{2\pi} = \frac{524 \text{ rad/s} \times 0.567 \text{ Wb}}{2\pi} = 47.3 \text{ V}.$$

The internal resistance of the 10-MJ HPG is 18.8 μΩ. Doubling this value as a first estimate for total circuit resistance gives a damping factor of

$$\zeta = \frac{R}{2\sqrt{L/C}} = 0.46$$

where R = total circuit resistance
L = total circuit inductance
C = machine equivalent capacitance.

This indicates that the inductor charging circuit will be underdamped. The time to peak current is then

$$t_{peak} = \frac{\tan^{-1}\left(\frac{2L\sqrt{\frac{1}{LC} - \frac{R^2}{4L^2}}}{R}\right)}{\sqrt{\frac{1}{LC} - \frac{R^2}{4L^2}}}.$$

The expression for the current is

$$I = \frac{V_{oc}}{L\sqrt{\frac{1}{LC} - \frac{R^2}{4L^2}}} \exp\left(\frac{-t/2L}{R}\right) \sin\sqrt{\frac{1}{LC} - \frac{R^2}{4L^2}}\ t$$

By iterating between these two equations, the value of coil resistance that will produce a peak discharge current of 750 kA is found to be approximately 5.7 μΩ. This is the average resistance of the coil during charging. The joule heating of the coil and the diffusion of current into the conductor during the transient must be accounted for in the coil design. The first effect raises the resistance of the circuit because of the dependence of resistivity on temperature. The second effect raises the circuit resistance because only the penetrated fraction of the conductor is utilized, making the transient resistance of the coil allowable tangential stress in the banding hoop due to a 3.45×10^7 N/m^2 (5,000 psi) internal pressure was taken as the maximum tensile stress for the banding, 3.79×10^8 N/m^2 (55,000 psi). The required thickness of banding is therefore

$$t = \frac{Pr_o}{\sigma} = \frac{5{,}000 \times 16 \text{ in.}}{55{,}000} \times \frac{2.54 \text{ cm}}{1 \text{ in.}}$$

$$= 3.68 \text{ cm } (1.45 \text{ in.})$$

Magnetic Shield Design

A quarter-section model of the coil with the shield simplified to a square structure was analyzed with a steady-state two-dimensional finite element code.[4] The maximum flux density change across the shield was 2.25 T. The maximum magnetic pressure seen on the walls of the shield is

$$\frac{1}{2}\int \frac{B^2}{\mu}\, dv = \int P\, dv$$

$$P = \frac{(2.25 \text{ V-s/m}^2)^2}{2(4\pi \times 10^{-7} \text{ V-s/A-m})}$$

$$= 2 \times 10^6 \text{ N/m}^2 \text{ (291 psi)}.$$

The shield structure is shown in Fig. 6. The hexagonal side walls are 91.4 cm wide x 189.9 cm high x 2.54 cm thick (36 x 72 x 1-in.) steel plate. The load on the side plates is therefore $F = 3.36 \times 10^6$ N (754,272 lb_f).

The magnetic load on the shield plates was supported by laminated wood ring girders and the 4-in. angle what attaches the wall to the base and the roof.

Coil Fabrication

The coil was wrapped about a fiberglass mandrel. The process was a simple one using mechanical screws reacting against a squirrel cage framework to bend the three conductors around the mandrel. The springback was addressed by clamping the individual conductors to the mandrel immediately behind the push station. Once secured, the push screws were backed off and the bending fixture was unclamped, rotated, and resecured. All during the winding, Nomex paper was applied to one side of each conductor to provide turn-to-turn and start-to-start insulation. When the bending was complete, the coil was cinched about its midsection with a Nylon cargo strap, and the first banding passes were applied above and below the strap. The strap was then removed, and the banding was completed. The banding was built up in several layers with a cure cycle between applications. Round aluminum plates were welded to the six input and output starts to complete the coil.

Comparison between Model and Full-size System

The resistance predicted by the model agrees well with the values measured in the full-size system, but the inductances do not agree as well (see Table 4). One difference is that the model coil was banded by hand, and the coil dimension "a" in Table 2 came out larger than desired. The large coil, on the other hand, was banded with a machine-controlled tension of 2,200 N (500 lb_f) and could be seen to tighten as the banding was applied. Equation 2 predicts a larger value of inductance for a loosely-wound coil, and this is what was measured.

Table 4. Comparison between Model and Full-size System

	Model	Model Scaled	Full-size System
Coils at 77 K in Shield			
Time to peak, ms	1.59	408	340
Resistance, μΩ	159	9.9	10.4
Inductance, μH	0.88	14	10
Coils at Room Temperature in Shield			
Time to peak, ms	1.41	361	300
Resistance, μΩ	669	41.8	45.8
Inductance, μH	0.9	14.4	10.8

References

1. Brooks, H. B., "Design of Standards of Inductance, and Proposed Use of Model Reactors in Design of Air-Core and Iron-Core Reactors," Bur. Stds. J. Res., 7 (2) Aug. 1931, 289-294.
2. Marshall, R. A., unpublished notes, Sept. 1981.
3. Bird, W. L., et al., Application of Rotating Energy Machines for Prime Energy Stores for Particle Beam Accelerators," Sandia Natl. Labs. Contract No. 26-2642, Sept. 1982.
4. Pillsbury, R. D., Texas Magnetic Analysis Program (TEXMAP) User's Manual, 1977.

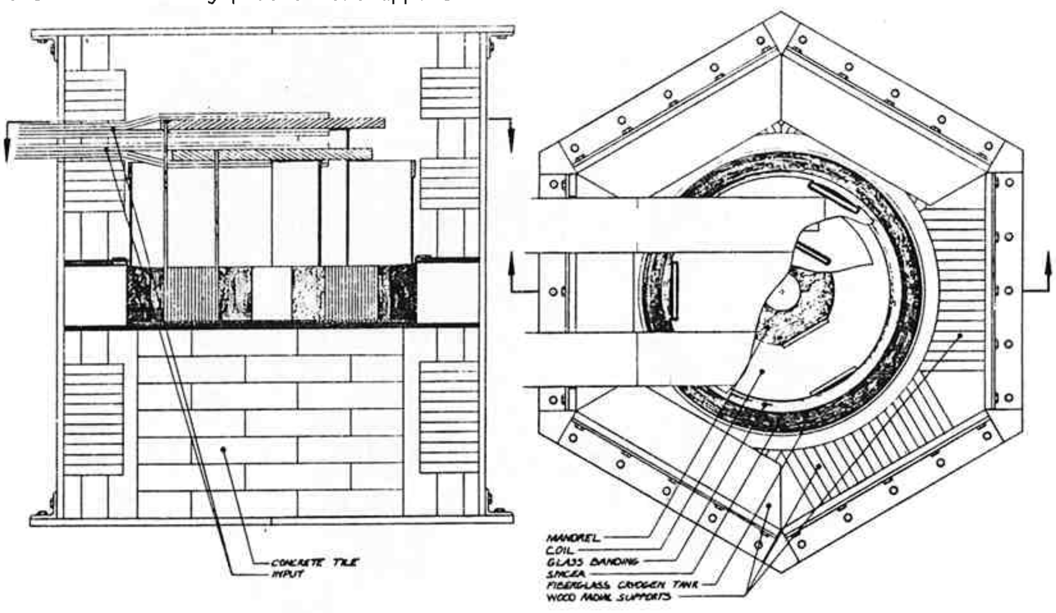

Fig. 6. Energy storage inductor and magnetic shield structure